The Plant Cell, Vol. 23: 1573–1587, April 2011, www.plantcell.org

Arabidopsis ABERRANT PEROXISOME MORPHOLOGY9 Is a Peroxin That Recruits the PEX1-PEX6 Complex to Peroxisomes [W]

Shino Goto,[a,b] Shoji Mano,[a,b] Chihiro Nakamori,[a] and Mikio Nishimura[a,b,1]

[a] Department of Cell Biology, National Institute for Basic Biology, Okazaki 444-8585, Japan
[b] Department of Basic Biology, School of Life Science, Graduate University for Advanced Studies, Okazaki 444-8585, Japan

Peroxisomes have pivotal roles in several metabolic processes, such as the detoxification of H_2O_2 and β-oxidation of fatty acids, and their functions are tightly regulated by multiple factors involved in peroxisome biogenesis, including protein transport. This study describes the isolation of an embryonic lethal *Arabidopsis thaliana* mutant, *aberrant peroxisome morphology9* (*apem9*), which is compromised in protein transport into peroxisomes. The *APEM9* gene was found to encode an unknown protein. Compared with *apem9* having the nucleotide substitution, the knockdown mutants showed severe defects in peroxisomal functions and plant growth. We showed that expression of *APEM9* altered PEROXIN6 (PEX6) subcellular localization from the cytosol to peroxisomes. In addition, we showed that PEX1 and PEX6 comprise a heterooligomer and that this complex was recruited to peroxisomal membranes via protein–protein interactions of APEM9 with PEX6. These findings show that APEM9 functions as an anchoring protein, similar to Pex26 in mammals and Pex15p in yeast. Interestingly, however, the identities of amino acids among these anchoring proteins are quite low. These results indicate that although the association of the PEX1-PEX6 complex with peroxisomal membranes is essential for peroxisomal functions, the protein that anchors this complex evolved uniquely in plants.

INTRODUCTION

Peroxisomes are single membrane-bound organelles that are ubiquitous in eukaryotic cells. Plant peroxisomes are differentiated into several types, including glyoxysomes, leaf peroxisomes, cotyledonary peroxisomes, root peroxisomes, and unspecialized peroxisomes (Kamada et al., 2003), and their functions are adapted in response to environmental and developmental cues (Nishimura et al., 1993). Glyoxysomes are responsible for the degradation of fatty acids, which provides the energy for postgerminative growth of seedlings. Leaf peroxisomes contain the enzymes that function in the glycolate pathway, which is active during photorespiration. Studies of various *Arabidopsis thaliana* mutants with defects in peroxisomal function demonstrated that peroxisomal function and biogenesis are essential for plant growth (Lin et al., 1999; Hayashi et al., 2002; Hu et al., 2002; Schumann et al., 2003; Sparkes et al., 2003; Zolman and Bartel, 2004; Fan et al., 2005; Hayashi and Nishimura, 2006; Mano et al., 2006; Kamigaki et al., 2009). Moreover, recent studies revealed that peroxisomes have functions such as polyamine catabolism in root cells (Kamada-Nobusada et al., 2008) and cuticular wax biosynthesis that are mediated via interaction with the endoplasmic reticulum (Kamigaki et al., 2009). In addition, use of plant genome information and proteomic approach using isolated peroxisomes identified novel peroxisomal functions in plants (Reumann et al., 2004, 2007; Arai et al., 2008; Eubel et al., 2008; Babujee et al., 2010).

Because peroxisomal proteins are encoded in the nuclear genome and transcribed in the cytosol, it is crucial that newly synthesized peroxisomal proteins are correctly transported into peroxisomes. Several peroxisome biogenesis factors, termed PEROXINs (PEXs), are involved in the transport of peroxisomal proteins from the cytosol to peroxisomes (Distel et al., 1996; Nito et al., 2007; Platta and Erdmann, 2007; Brown and Baker, 2008). Most peroxisomal matrix proteins are synthesized in the cytosol and then transported to peroxisomes when their peroxisomal targeting signals (PTS1 and PTS2) are recognized by PEX receptors (PEX5 and PEX7, respectively), which travel to the peroxisomal membrane (Kragler et al., 1998; Zolman et al., 2000; Nito et al., 2002; Hayashi and Nishimura, 2006; Platta and Erdmann, 2007). In plants, PEX5 interacts with PEX7 in the cytosol, and the PEX5-PEX7 complex containing matrix proteins is recognized by the transport machinery, which includes PEX14, on the peroxisomal membranes (Nito et al., 2002; Singh et al., 2009; Khan and Zolman, 2010). In yeast (such as *Saccharomyces cerevisiae* and *Pichia pastoris*) and mammals, it has been demonstrated that, after cargo proteins are released from the receptors inside peroxisomes, the receptors are recycled to the cytosol for a new round of protein import. This recycling system requires another set of PEXs, including RING finger proteins, PEX2, PEX10, and PEX12; the E2 ubiquitin-conjugating enzyme PEX4; PEX22, which anchors PEX4 to the peroxisomal membrane; and the AAA-ATPase PEX1-PEX6 complex (Collins et al., 2000; Nair et al., 2004; Miyata and Fujiki, 2005; Zolman et al., 2005; Platta et al., 2007). Of them, the

[1] Address correspondence to mikosome@nibb.ac.jp.
The author responsible for distribution of materials integral to the findings presented in this article in accordance with the policy described in the Instructions for Authors (www.plantcell.org) is: Mikio Nishimura (mikosome@nibb.ac.jp).
[W] Online version contains Web-only data.
www.plantcell.org/cgi/doi/10.1105/tpc.110.080770

PEX1-PEX6 complex, which has no transmembrane domain (TMD), was reported to be tethered to peroxisomal membranes via protein–protein interactions with peroxisomal membrane proteins Pex26 and Pex15p in mammals and yeast, respectively (Elgersma et al., 1997; Geisbrecht et al., 1998; Faber et al., 1998; Birschmann et al., 2003; Matsumoto et al., 2003). However, the mechanism on targeting of PEX1 and PEX6 to peroxisomes and the presence of PEX1-PEX6 complex remains to be clarified in plant cells.

Although these factors that are thought to be involved in peroxisomal protein transport have been determined in plants (Mullen et al., 2001; Zolman et al., 2005; Nito et al., 2007), the details of the molecular interactions are not completely understood. In addition, some factors, such as Pex8, Pex17, and Pex15/Pex26, that have been identified as being important in peroxisomal protein transport in yeast and mammals are not present in plant genomes (Faber et al., 1998; Geisbrecht et al., 1998; Huhse et al., 1998; Rehling et al., 2000; Brown and Baker, 2008; Meinecke et al., 2010). This indicates either that plants do not have the same peroxisomal protein transport system as yeast and mammals or that it is difficult to detect plant homologs of yeast and mammalian PEXs due to low levels of similarity.

Previously, we screened transgenic *Arabidopsis* plants that express peroxisome-targeted green fluorescent protein (GFP-PTS1 plants) for mutants defective in peroxisome biogenesis and function (Mano et al., 2002). We isolated several *aberrant peroxisome morphology* (*apem*; previously called *apm*) mutants that have different GFP fluorescence patterns from those of parental GFP-PTS1 plants (Mano et al., 2004, 2006). In this study, we report the identification of APEM9 as a peroxisome biogenesis factor in plants, based on an analysis of the *Arabidopsis apem9* mutant, which exhibited a defect in peroxisomal protein transport. We revealed that APEM9 interacts with PEX6 and is required for the peroxisomal localization of the AAA-ATPase PEX1-PEX6 complex. Judging from these results, APEM9 has a similar function like mammalian Pex26 and yeast Pex15p, although the identities of amino acids among APEM9, Pex26, and Pex15p were quite low. *apem9* mutants were defective in peroxisomal function due to defects in peroxisomal protein transport. As a result, normal plant growth, including seed germination and embryo development, was disturbed in *apem9* mutants.

RESULTS

Isolation of the *apem9* Mutant

As reported previously, we isolated a number of *apem* mutants among transgenic *Arabidopsis* plants expressing GFP-PTS1 that had different patterns of GFP fluorescence from the parental GFP-PTS1 plants (Mano et al., 2004, 2006). In parental GFP-PTS1 plants, GFP fluorescence was observed as punctate peroxisomal signals in most cells (Figure 1A, left panels). By contrast, GFP fluorescence was detected in the cytosol as well as in peroxisomes of *apem9-1* mutants (Figure 1A, right panels). This *apem9-1* phenotype was exclusively observed in leaf trichomes, root epidermal cells, and root hairs and was not present in most tissues, such as leaf epidermis or internal cells

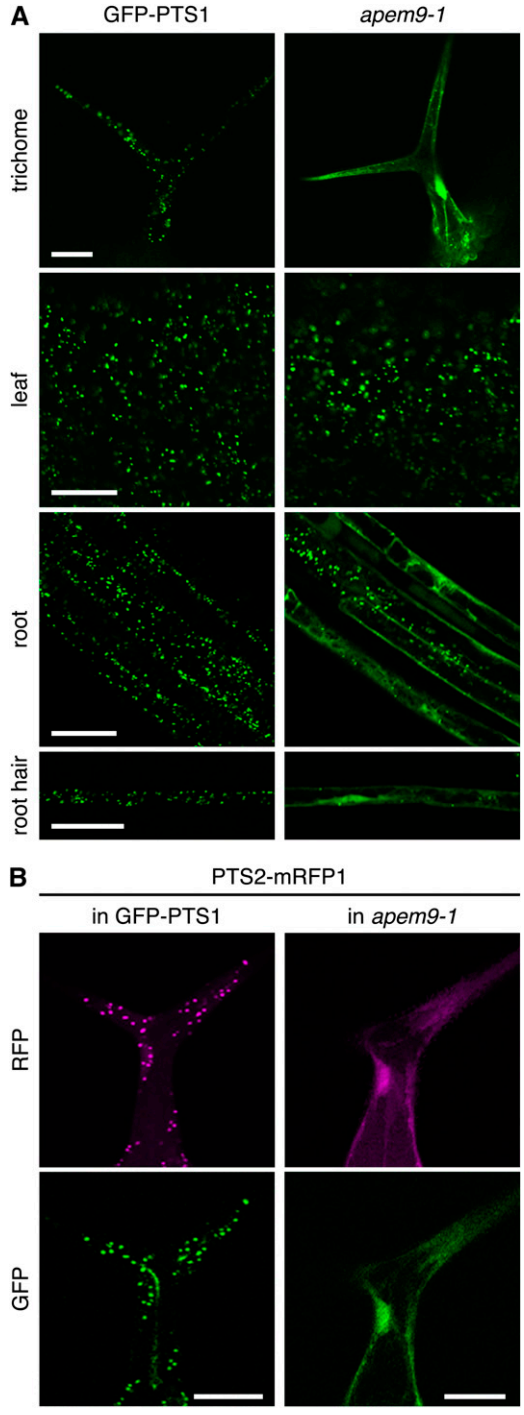

Figure 1. The *apem9-1* Phenotype.

(A) GFP fluorescence patterns of the parental GFP-PTS1 plants and *apem9-1* mutants. The indicated tissues of 2-week-old plants were examined using confocal laser scanning microscopy.

(B) The efficiency of PTS2-dependent protein transport in *apem9-1* plants. *PTS2-mRFP1* was introduced into GFP-PTS1 plants (left panels) and *apem9-1* (right panels) mutants. Images show the trichomes of 2-week-old plants.

Bars = 50 μm.

(mesophyll and root cortex cells). Since GFP is transported into peroxisomes via a PTS1-dependent pathway, the presence of GFP fluorescence in the cytosol of *apem9-1* cells suggests that APEM9 is involved in PTS1-dependent protein transport. The nonuniformal GFP fluorescence phenotype was also observed in other mutants, *pex13* (previously called *apm2*) and *pex12* (previously called *apm4*), which show defects in protein transport (Mano et al., 2006). This phenotype might be due to the different activity of protein transport between the different types of cells, in which requirement of APEM9 differs. Additionally, the plant growth of *apem9-1* mutants is not suppressed dramatically (see Figures 9C and 9D), supporting that the *apem9-1* is a leaky allele.

To examine the effect(s) of the *apem9-1* mutation on the PTS2-dependent pathway, a second mechanism for protein transport to peroxisomes (Hayashi and Nishimura, 2006), we generated transgenic plants in which the PTS2-mRFP1 fusion protein was expressed in the GFP-PTS1 plants or *apem9-1* mutants. In the GFP-PTS1 plants, the red fluorescent protein (RFP) signal was observed only in peroxisomes (Figure 1B, top left), whereas it was diffusely distributed throughout the cytosol in the *apem9-1* mutants (Figure 1B, top right). In the *apem9-1* mutants, the pattern of mislocalization of PTS2-mRFP1 protein corresponded to that of GFP-PTS1 protein (Figure 1B). These results show that APEM9 is involved in both PTS1- and PTS2-dependent protein transport.

Identification of the *APEM9* Gene

All the first filial (F1) progenies from the crossing of the *apem9-1* plant with the GFP-PTS1 plant displayed a punctate GFP fluorescence phenotype like GFP-PTS1 plants, and no F1 progenies displayed cytosolic GFP fluorescence like *apem9-1* mutants (wild type:*apem9-1* = 60:0). The second filial (F2) progenies segregated into the punctate and cytosolic GFP fluorescence phenotypes (wild type:*apem9-1* = 33:7), indicating that the *apem9-1* mutation segregates as a monogenic recessive gene. The *APEM9* gene was mapped between F13M14 and T713 BAC clones on chromosome 3 using map-based cloning. We found that a single nucleotide substitution of G to A in *At3g10572*, which encodes a protein consisting of 333 amino acids (Figures 2A and 2B). The *apem9-1* mutation results in the substitution of Gly-278 with Glu (G278E). The identification of the mutation responsible for the *apem9-1* phenotype was confirmed by the following two experiments. First, a genomic DNA fragment, bearing *At3g10572* with 1.8 kb upper region from start codon and 0.5 kb downstream region from stop codon, was introduced into *apem9-1* mutants (Figure 2C). GFP fluorescence was observed only in the peroxisomes of *apem9-1* T1 plants transformed with this genomic DNA fragment, as observed in GFP-PTS1 plants. This result shows that *At3g10572* expression is sufficient to rescue the *apem9-1* phenotype. Next, we crossed *apem9-1* mutants with T-DNA insertion lines to test whether these lines are allelic to the *apem9-1* mutant. Two lines with a T-DNA insertion in the *At3g10572* locus, SALK_132193 and SALK_022380 that were designated *apem9-2* and *apem9-3*, respectively, were identified using the SIGnAL T-DNA Express: Arabidopsis Gene Mapping Tool (Figure 2A; Alonso et al., 2003). *apem9-2* and *apem9-3* contained a T-DNA insertion in exon 5 or 2 of *At3g10572* gene, respectively. Unfortunately, we could not obtain homozygous *apem9-2* or *apem9-3* mutants as mentioned below. Therefore, heterozygotes (*apem9-2*/+ or *apem9-3*/+) were used for crossing with *apem9-1*. As shown in Figure 2D, the F1 progeny harboring the *apem9-1* mutation and T-DNA insertion accumulated GFP fluorescence in the cytosol, as did the *apem9-1* mutants. In addition, the cytosolic fluorescence was expanded in epidermal cells of cotyledons in heterozygotes (Figure 2D). Thus, neither of the T-DNA insertion alleles could complement the *apem9-1* phenotype. From these results of complementation and allelism tests, we concluded that the *APEM9* gene is *At3g10572*.

A review of public databases found that *At3g10572* has been annotated as 3-phosphoinositide-dependent protein kinase-1, putative. This annotation was originally provided for the predicted gene F18K10.16 (accession number AAF76360), which is on a locus that contains two genes, *At3g10572* and *At3g10575*. At present, *At3g10572* and *At3g10575* are considered to be distinct genes, and *At3g10575* is further regarded to be a pseudogene. Of these genes, *At3g10575*, but not *At3g10572*, is similar to the rice gene annotated as 3-phosphoinositide-dependent protein kinase-1, putative (accession number BAB86551). Therefore, we concluded that the current annotation in the database does not apply to *At3g10572*. In addition, we found that no functional domains are predicted to occur in the primary amino acid sequence of APEM9, indicating that APEM9 is a functionally unknown protein.

Peroxisomal Localization of APEM9

Using the applications for TMD prediction, one or two TMDs were predicted to occur in the N-terminal and C-terminal hydrophobic region of APEM9 (corresponding to amino acids 91 to 102 and 273 to 284, respectively). Of these two regions, we assumed that the C-terminal region is a possible TMD with high-predicted score (Figure 3A). The observation that the *apem9-1* mutation, G278E, is located in this TMD suggests that the mutation affects APEM9 localization. This hypothesis is further supported by the fact that some peroxisomal membrane proteins contain localization information in their TMD (Rottensteiner et al., 2004). Therefore, we attempted to determine the subcellular localization of the wild-type and mutant forms of APEM9. The *GFP-APEM9* fusion gene, which is controlled by the constitutive cauliflower mosaic virus (CaMV) 35S promoter, was transiently expressed in onion (*Allium cepa*) epidermal cells using particle bombardment. GFP-APEM9 was observed as rapidly moving punctate structures (Figure 3B, left). To confirm the peroxisomal localization of APEM9 in *Arabidopsis*, this fusion gene was transiently expressed in *Arabidopsis* cells. The same result was obtained: TagRFP-fusion APEM9 accumulated in peroxisomes of *Arabidopsis* cells (see Supplemental Figure 1A online). To determine the suborganellar localization of APEM9, we simultaneously expressed *GFP-APEM9* and *mRFP1-PTS1*, a peroxisomal matrix marker, in onion epidermal cells. The GFP-APEM9 signal (green) was observed as ring-like structures (Figure 3C, left) surrounding the RFP-labeled matrix (Figure 3C, middle and right), showing that APEM9 is targeted to peroxisomal membranes. Interestingly, a fusion protein of GFP with APEM9

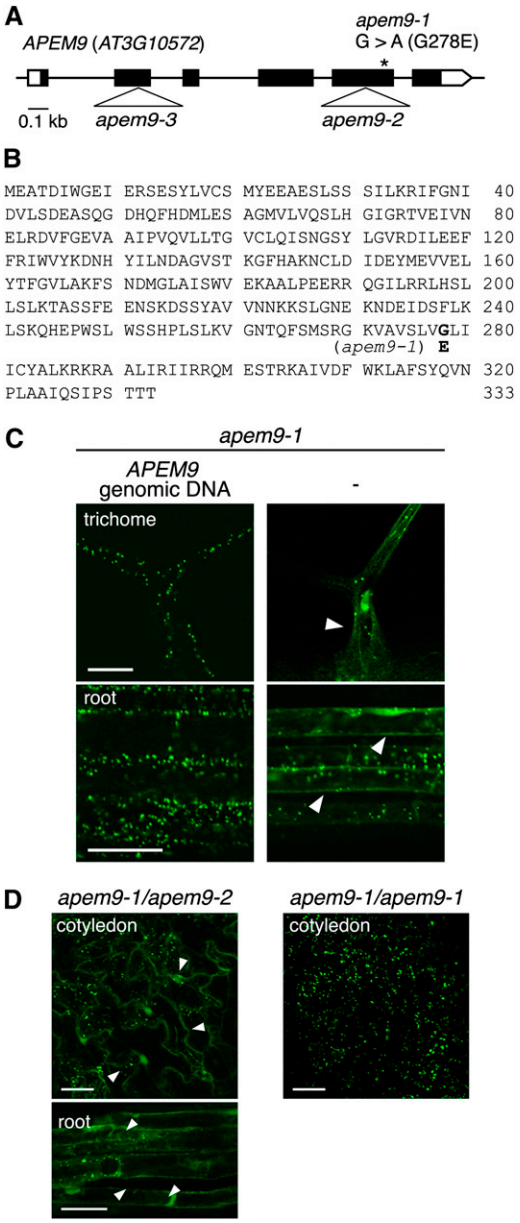

Figure 2. Identification of the *APEM9* Gene.

(A) Schematic structure of *APEM9*. The white and black boxes indicate untranslated regions and exons, respectively. An asterisk represents the location of the nucleotide substitution in *apem9-1*, which changes the guanine residue at position 1701 to adenine (where nucleotide 1 corresponds to the adenine residue of the first Met codon), causing an amino acid substitution of Gly-278 to Glu. The positions of the T-DNA insertion in the *apem9-2* and *apem9-3* lines are indicated by triangles.

(B) Amino acid sequence of the APEM9 protein. The bold G represents Gly-278, which is replaced by Glu (bold E) in the *apem9-1* mutant.

(C) *At3g10572* restored the GFP fluorescence pattern in *apem9-1* plants. Images show *apem9-1* trichome and root cells transformed with *At3g10572* (left column) or not transformed (right column). Two-week-old seedlings were examined by confocal laser scanning microscopy. White arrowheads indicate the cells exhibiting the *apem9-1* phenotype. Bars = 50 μm.

(D) Test of allelism between *apem9* alleles. GFP fluorescence patterns in the F1 progeny, which was derived from crossing *apem9-1* with *apem9-2*, were compared with *apem9-1* (*apem9-1/apem9-1*). The cotyledons and roots of 2-week-old seedlings were examined. White arrowheads indicate the cells exhibiting the *apem9-1* phenotype. Bars = 50 μm.

containing the *apem9-1* mutation, GFP-APEM9$^{[G278E]}$, was not localized to peroxisomes but was diffusely distributed in the cytosol (Figure 3B, right). Thus, the Gly-278 residue is important for APEM9 localization to the peroxisomal membrane.

APEM9 Is Required for the Peroxisomal Localization of PEX6 but Not PEX1

Based on our microscopy observations, we speculated that APEM9 is a component of the transport machinery complex, which consists of several PEXs. Most of these PEXs are membrane proteins that function at peroxisomal membranes (Brown and Baker, 2008). However, the AAA-ATPase PEX1-PEX6 complex, which has no TMD, was reported to be directed to peroxisomal membranes via protein–protein interactions with PEX6 and the peroxisome-localized anchoring proteins, Pex26 (Geisbrecht et al., 1998; Matsumoto et al., 2003) and Pex15p (Faber et al., 1998; Birschmann et al., 2003) in mammals and yeast, respectively. In plants, PEX1 and PEX6 are also important for peroxisome biogenesis because defects in the *Arabidopsis* homologs of PEX1 and PEX6 confer severe defects in protein transport (Zolman and Bartel, 2004; Nito et al., 2007). However, the mechanism by which proteins are targeted to peroxisomes via PEX1 and PEX6 in plant cells remains to be clarified. Therefore, we examined the influence of APEM9 on the subcellular localization of PEX1 and PEX6. We constructed *TagRFP-PEX6* and *TagRFP-PEX1* fusion genes for transient expression in onion epidermal cells. When *TagRFP-PEX6* was expressed alone, the RFP signal was observed in the cytosol, but not as punctate particles (Figure 4A). To exclude the possibility that the cytosolic localization of PEX6 is due to the heterologous expression of *Arabidopsis* PEX6 in onion cells, this fusion gene was transiently expressed in *Arabidopsis* cells. The same result was obtained: TagRFP-PEX6 accumulated in the cytosol of *Arabidopsis* cells (see Supplemental Figure 1B online). When the *TagRFP-PEX6* and *GFP-APEM9* constructs were simultaneously expressed in onion epidermal cells, RFP signal was observed as punctate structures, as was the GFP signal (Figure 4B). These two signals were detected as ring-like structures that perfectly overlapped (Figure 4C), indicating that GFP-APEM9 redirected TagRFP-PEX6 from the cytosol to peroxisomal membranes. However, when GFP-APEM9$^{[G278E]}$ was used instead of GFP-APEM9, TagRFP-PEX6 remained in the cytosol (Figure 4D). Therefore, APEM9 is required for PEX6 transport from the cytosol to peroxisomal membranes. The fluorescence from transiently expressed TagRFP-PEX6 was detected in the cytosol (Figure 4A; see Supplemental Figure 1B online), and it did not seem that TagRFP-PEX6 was affected by endogenous APEM9. This might be caused due to an imbalance of a small amount of endogenous APEM9 to a high amount of TagRFP-PEX6 in cells, and the faint signal from peroxisomal membrane might be masked by intense

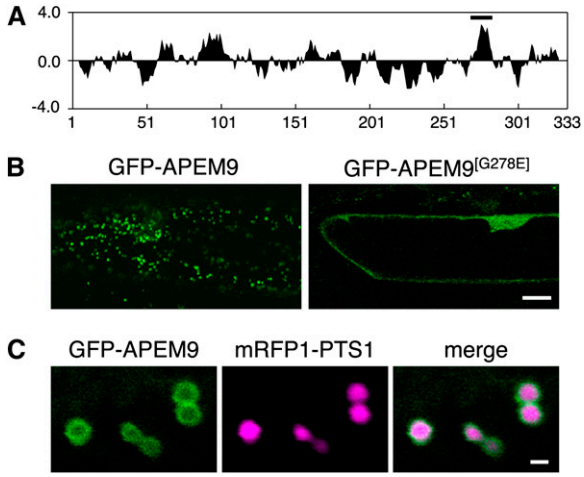

Figure 3. APEM9 Localizes to the Peroxisomal Membrane.

(A) Hydropathy profile of APEM9. Hydrophobic and hydrophilic residues are depicted as positive and negative values, respectively, using the Kyte and Doolittle scale. The bar above the plot indicates the hydrophobic region that contains a transmembrane domain, as predicted by the DAS TM-filter (http://mendel.imp.ac.at/sat/DAS/DAS.html).

(B) Subcellular localization of the APEM9 protein and effect of the *apem9-1* mutation on APEM9 protein localization. GFP fusions of the wild-type *APEM9* (left) and the *APEM9*$^{[G278E]}$ mutant (right) were transiently expressed in onion epidermal cells. Bar = 20 μm.

(C) Magnified images of the punctate structure as shown in **(B)**, left. *GFP-APEM9* was introduced into onion epidermal cells with a peroxisomal marker, *mRFP1-PTS1*, using the particle bombardment system. GFP and mRFP1 signals were observed using confocal laser scanning microscope. Bar = 1 μm.

cytosolic fluorescence. When additional APEM9 was supplied by overexpression (Figure 4B), most TagRFP-PEX6 could be moved to peroxisomal membrane, and TagRFP-fluorescence was detected on peroxisomes. When *TagRFP-PEX1* was expressed alone, the fluorescence was observed in the cytosol (Figure 4E), as was the case for *TagRFP-PEX6*. In contrast with PEX6, however, the subcellular localization of TagRFP-PEX1 was not altered by *GFP-APEM9* coexpression (Figure 4F). Hence, APEM9 directly affects the localization of PEX6 but not of PEX1.

Protein–Protein Interactions among APEM9, PEX6, and PEX1

To study the interaction between APEM9 and PEX6, we performed a bimolecular fluorescence complementation (BiFC) assay (Bracha-Drori et al., 2004; Singh et al., 2009). For this assay, constructs expressing the fusion proteins nYFP-PEX6 and cYFP-APEM9 were generated, in which PEX6 and APEM9 were fused to the N- and C-terminal fragments of yellow fluorescent protein (YFP), respectively. *nYFP-PEX6* and *cYFP-APEM9* were simultaneously expressed in onion epidermal cells together with a peroxisome marker, *mRFP1-PTS1*. As shown in Figure 5A, the reconstituted YFP fluorescence was detected as punctate signals that overlapped with RFP-labeled peroxisome signals, and highly magnified images displayed the YFP signals as ring-like structures surrounding peroxisomal RFP signals (see Supplemental Figure 1C online). These results indicate that APEM9 interacts with PEX6. Interestingly, weak YFP fluorescence was observed when the combination of the mutant form APEM9$^{[G278E]}$ and PEX6 was tested (Figure 5B). However, this YFP signal was observed in the cytosol and not in peroxisomes. Thus, APEM9$^{[G278E]}$ retains the ability to interact with PEX6 but not to recruit it to peroxisomes because APEM9$^{[G278E]}$ itself cannot localize to peroxisomal membranes.

The AAA-ATPases, PEX1 and PEX6, constitute hetero-oligomers that function in yeast (Faber et al., 1998) and mammalian cells (Geisbrecht et al., 1998; Tamura et al., 2006). To examine whether PEX1 and PEX6 are able to interact in plant cells, we produced a *cYFP-PEX1* fusion construct for use in a BiFC assay. The *nYFP-PEX6* and *cYFP-PEX1* fusion genes were simultaneously expressed, together with *mRFP1-PTS1*, in onion epidermal cells. As shown in Figure 5F, the reconstituted YFP signal was detected diffusely in the cytosol, a distribution significantly different from that of the punctate mRFP1-PTS1 signals, showing that PEX6 interacts with PEX1 and that this complex accumulates in the cytosol. By contrast, when *TagRFP-APEM9* was simultaneously expressed with *nYFP-PEX6* and *cYFP-PEX1*, YFP signal was observed predominantly in peroxisomes, which were marked with TagRFP-APEM9 (Figure 5G). We carefully examined cells expressing negative controls to exclude the possibility that YFP molecules were accidentally reconstituted (Figures 5C to 5E and 5H). To rule out the possibility of nonspecific interactions occurring due to random collisions on the peroxisomal membrane, combinations with other membrane proteins, PMP38 and PEX12, were tested. No interactions were detected using these negative controls (Figures 5I and 5J; Fukao et al., 2001; Mano et al., 2006).

Pex19 is reported to be required for targeting of peroxisomal membrane protein transport (Rottensteiner et al., 2004; Shibata et al., 2004; Schueller et al., 2010). In Figure 5K, *nYFP-PEX19-1* and *cYFP-APEM9* were introduced with a peroxisomal marker, *mRFP1-PTS1*. YFP fluorescence was predominantly observed in particles and aggregated vesicles, which completely overlapped with the RFP signal. In addition, a small amount of YFP signal was also detected in the cytosol. This result implicates that APEM9 is transported to peroxisomes via the interaction with PEX19, like other peroxisomal membrane proteins.

The results of the BiFC assay demonstrated the specificity of the interaction between APEM9-PEX6 and PEX6-PEX1. To confirm the interaction between APEM9 and PEX6, we performed a comprehensive interaction analysis using the mating-based split ubiquitin system (mbSUS), which can detect interactions of membrane proteins with other membrane proteins (Ludewig et al., 2003; Obrdlik et al., 2004; Grefen et al., 2007). For this assay, constructs expressing the fusion proteins Nub-tagged *APEM9*, *APEM9*$^{[G278E]}$, or *PMP38* and Cub-PLV–tagged *PEX6* were generated, in which Nub and Cub represent the N- and C-terminal fragments of ubiquitin, respectively (Figure 6). Yeast cells expressing *APEM9-Nub* with *Cub-PLV-PEX6* (Figure 6, lane 1) and *APEM9*$^{[G278E]}$*-Nub* with *Cub-PLV-PEX6* (Figure 6, lane 2) could grow on interaction selection medium (Figure 6, bottom panel), where the reconstitution of halves of ubiquitin (Nub and Cub) results in the cleavage of the PLV peptide, causing

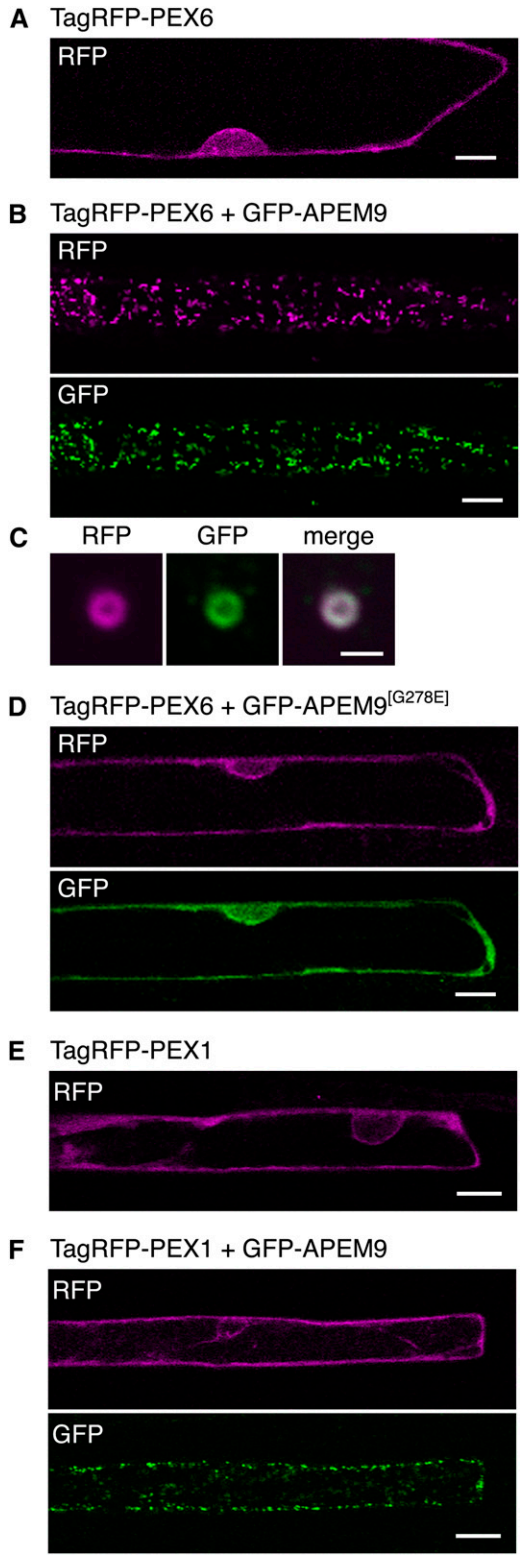

Figure 4. APEM9 Is Required for Peroxisomal Localization of PEX6, but Not PEX1.

(A) to **(D)** Subcellular localization of PEX6.
(A) Expression of *TagRFP-PEX6* alone. Bar = 20 μm.
(B) Coexpression of *TagRFP-PEX6* with *GFP-APEM9*. Bar = 20 μm.
(C) Magnified images of a punctate structure as shown in **(B)**. Bar = 1 μm.
(D) Coexpression of *TagRFP-PEX6* with *GFP-APEM9*$^{[G278E]}$. Bar = 20 μm.
(E) and **(F)** Subcellular localization of PEX1. Expression of *TagRFP-PEX1* alone **(E)** or with *GFP-APEM9* **(F)**. Bars = 20 μm.

expression of genes for *Ade2* and *His3*. By contrast, yeast cells expressing *PMP38-Nub* with *Cub-PLV-PEX6* could not grow on interaction selection medium (Figure 6, lane 3), showing that the interaction of PMP38 with PEX6 did not occur. These results are good agreement with the data obtained in the BiFC assay of specific interactions of PEX6 with APEM9 and APEM9$^{[G278E]}$ but not with PMP38.

APEM9 Is an Anchoring Protein Uniquely Evolved in Plants

A BLAST search of public databases (GenBank/EMBL/DDBJ) found that no gene homologs of *APEM9* are present in mammals, yeast, and unicellular organisms. However, genes homologous to *Arabidopsis APEM9* are present in several plant genomes, including those of dicotyledonous and monocotyledonous species (see Supplemental Table 1 online). Additionally, we detected homologous genes in a fern and a moss, although they had low levels of similarity with *Arabidopsis APEM9*. These findings revealed that *APEM9* is a plant-unique gene.

We demonstrated that, like mammalian Pex26 and yeast Pex15p, APEM9 acts as an anchoring protein for the AAA-ATPase complex, which consists of PEX1 and PEX6, in plants. However, the amino acid sequences of APEM9, Pex26, and Pex15p share low levels of identity (<20%). Indeed, the level of identity is low even between Pex26 and Pex15p, which are known to be counterparts of each other (Birschmann et al., 2003; Matsumoto et al., 2003; Halbach et al., 2006). Interestingly, APEM9 homologs in plants, Pex26 homologs in mammals, and Pex15p homologs in yeast each have one TMD in their C-terminal region and have similar hydropathy profiles to each other (see Supplemental Figure 2A online). To determine whether each protein can function in other organisms, we performed a complementation analysis using *Arabidopsis APEM9* in a yeast mutant that lacks *Pex15p* (*pex15*). *pex15* knockout yeast cells cannot grow on plates containing oleate as a sole carbon source, as previously reported (Birschmann et al., 2003). APEM9 could not rescue this *pex15* mutant phenotype (see Supplemental Figure 2B online).

Next, we made a construct in which yeast Pex15p was fused to GFP at its N terminus and driven by the CaMV 35S promoter (GFP-ScPex15p). This construct was introduced into onion epidermal cells along with the peroxisomal marker, *mRFP1-PTS1*, using particle bombardment. Unlike in the case of GFP-APEM9 (Figure 3B), GFP signal was detected in the cytosol but not in peroxisomes labeled with mRFP1 (see Supplemental Figure 2C online). This result shows that yeast Pex15p is not targeted to peroxisomes in plant cells.

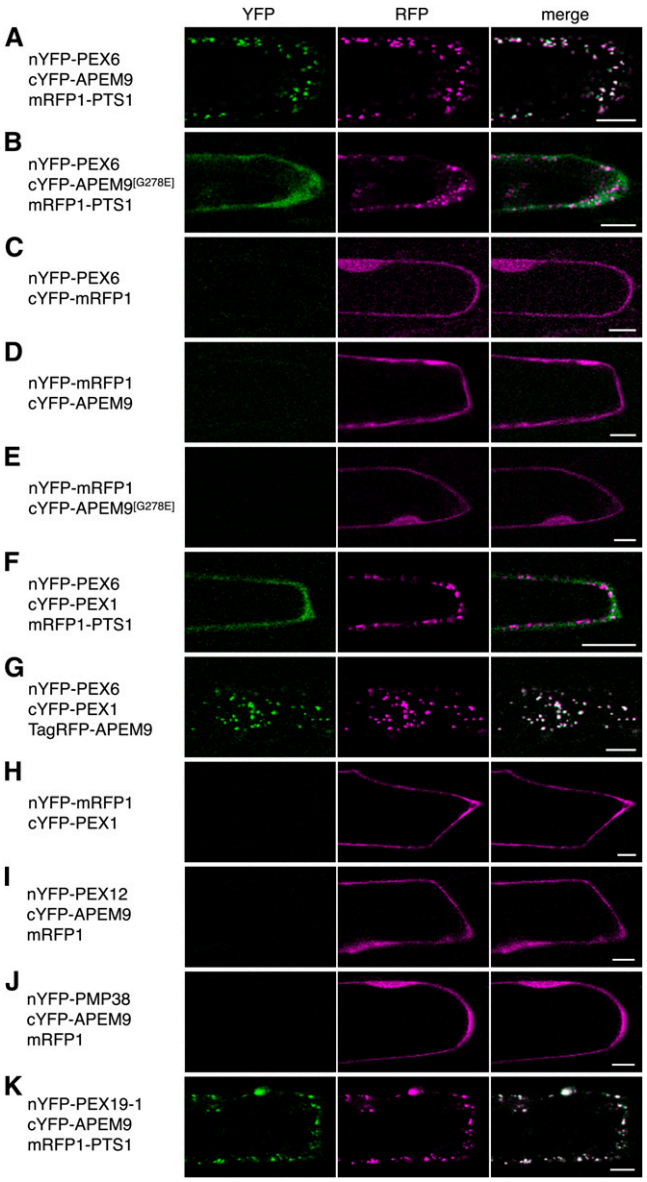

Figure 5. APEM9 Directs the Localization of the PEX1-PEX6 Complex to Peroxisomes.

Detection of protein–protein interactions using the BiFC assay. Onion epidermal cells were used for the transient expression of combinations of *nYFP* and *cYFP* fusion genes, as noted to the left of each panel. *mRFP1-PTS1* and *mRFP1* were used as markers of peroxisomes and of bombarded cells, respectively. **(C)** to **(E)** and **(H)** are negative controls, in which RFP fluorescence from nYFP-mRFP1 or cYFP-mRFP1 was detected to confirm the expression of the YFP fragment. **(I)** and **(J)** show detection of the interaction of APEM9 and the peroxisomal membrane proteins, PEX12 **(I)** or PMP38 **(J)**. **(K)** shows detection of the interaction between APEM9 and PEX19-1. YFP, RFP, and merge (top) represent YFP and RFP fluorescence and merged images, respectively. Bars = 20 μm.

APEM9 Gene Expression in *Arabidopsis*

Peroxisomes are involved in several metabolic processes throughout the plant life cycle, such as lipid metabolism and photorespiration (Hayashi and Nishimura, 2006). This suggests that APEM9 is also required during the entire plant life cycle. Therefore, we examined *APEM9* expression in various tissues at different developmental stages of wild-type plants. Quantitative RT-PCR analysis showed that the level of *APEM9* mRNA was almost constant in different tissues of *Arabidopsis* plants. In floral organs containing young buds and opened flowers, a little upregulated gene expression was detected, but there was no significance between other tissues (Figure 7). These results suggest that *APEM9* functions throughout the plant life cycle.

Defects in Seed Development in T-DNA Insertion Lines

We found that the T-DNA insertion lines, *apem9-2* and *apem9-3* (Figure 2A), do not produce homozygous seeds. Self-fertilized fruits from heterozygous *apem9-2* (*apem9-2*/+) or *apem9-3* (*apem9-3*/+) plants contain around 20% aborted seed, which are shrunken or translucent white (Figure 8). Because this phenotype is commonly observed in T-DNA insertion lines of the *Arabidopsis PEX2/TED3* (Hu et al., 2002), *PEX10* (Schumann et al., 2003; Sparkes et al., 2003), *PEX12* (Fan et al., 2005), and *PEX16/SSE1* (Lin et al., 1999) genes, we can conclude that *APEM9* has an important role in peroxisome biogenesis during the reproductive process.

Analysis of *APEM9* Knockdown Mutants, *apem9i*

Because the *apem9-1* phenotype was leaky and homozygotes of T-DNA insertion lines (*apem9-2* and *apem9-3*) were unobtainable, knockdown mutants (*apem9i*) were generated by the double-stranded RNA interference (RNAi) method (Figure 9A) to analyze the biological functions of APEM9. The vector, which generated double-stranded RNA corresponding to *APEM9* 1 to 171 bp coding region, was introduced into the GFP-PTS1 plants. From the 20 independent RNAi lines produced, four independent

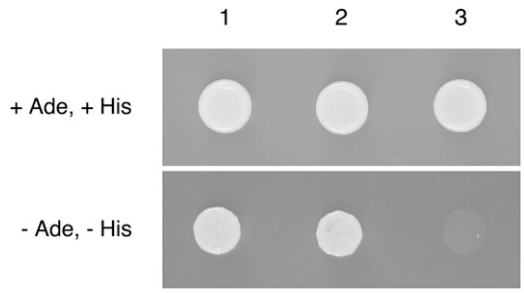

Figure 6. Detection of the Interaction between APEM9 and PEX6 by Yeast mbSUS Growth Assays.

Yeast THY.AP4 clones expressing Cub-PLV–tagged *PEX6* were mated with THY.AP5 clones expressing Nub-tagged *APEM9* (1), *APEM9*$^{[G278E]}$ (2), or *PMP38* (3) as a negative control. Growth of the diploid cells was tested on vector-selective (+Ade and +His) or interaction-selective (-Ade and -His) medium.

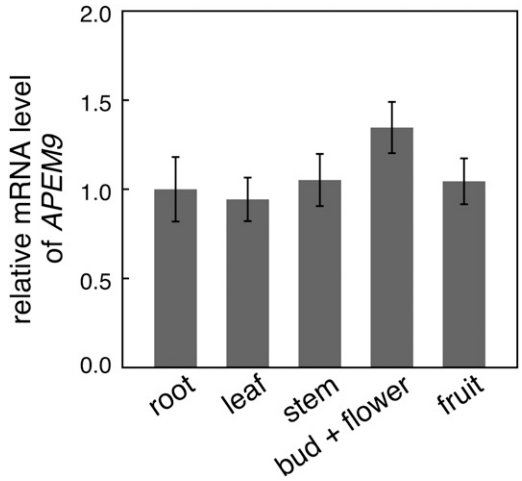

Figure 7. Expression Levels of *APEM9* in Various Tissues.

The amount of *APEM9* mRNA was determined by quantitative RT-PCR. Root mRNAs were prepared from 2-week-old plants and other tissues were from 7-week-old plants. The data are relative to the expression of *Ubiquitin 10* and were further normalized to the level of root mRNA, which is expressed as 1.0. Data are represented as means ± SE from three independent experiments.

lines, *apem9i* #3, #4, #8, and #15, which exhibited the strongest reduction in *APEM9* mRNA accumulation, were selected for physiological analysis (Figure 9B). Unlike the *apem9-1* mutants that exhibit no visible phenotype, the *apem9i* mutants had pale-green leaves and exhibited a dwarf phenotype (Figures 9C and 9D). The efficiency of PTS1-dependent protein transport in *apem9i* mutants was dramatically reduced compared with that of *apem9-1* mutants (cf. Figure 1A with Figure 9E). In contrast with the *apem9-1* phenotype, cytosolic GFP fluorescence was observed even in the leaf epidermis and root cortex of *apem9i* mutants (Figure 9E). To examine the effect on PTS2-dependent protein transport in *apem9i* plants, the *PTS2-mRFP1* construct, which is controlled by the constitutive CaMV 35S promoter, was transiently expressed in epidermal cells of the GFP-PTS1 plants and *apem9i* mutants using particle bombardment. In the GFP-PTS1 plants, the RFP signal was observed in peroxisomes, whereas it was diffused through the cytosol in the *apem9i* mutants (Figure 9F).

We performed subsequent immunoblot analysis to confirm the above localization result (Figure 9G). A PTS2-containing protein, 3-ketoacyl-CoA thiolase, is synthesized in the cytosol as a precursor form containing PTS2, and PTS2 is removed after the translocation of thiolase into peroxisomes (Preisig-Müller and Kindl, 1993; Kato et al., 1996). In GFP-PTS1 plants, only the mature form of thiolase is detected, whereas both the mature and precursor forms are detected in protein transport-defective mutants, such as *pex12/apm4* (Figure 9G; Mano et al., 2006). In *apem9i* mutants, 3-ketoacyl-CoA thiolase predominantly accumulated as the precursor form in the cytosol (Figure 9G). These results revealed that both PTS1- and PTS2-dependent protein transport is dramatically disturbed in *apem9i* mutants. Compared with *apem9i* mutants, mature form was predominantly accumulated in *apem9-1* mutants, like the GFP-PTS1 plants (Figure 9G). This is due to the leaky phenotype of *apem9-1*, in which a large population of cells displays normal peroxisomal protein transport.

To investigate the effects of defective APEM9 on significant peroxisomal functions, we determined the fatty acid β-oxidation activity of the *apem9* mutants. Peroxisomal fatty acid β-oxidation metabolizes 2,4-dichlorophenoxybutyric acid (2,4-DB) to produce an herbicide, 2,4-dichlorophenoxyacetic acid (Wain and Wightman, 1954; Hayashi et al., 1998). Peroxisomal fatty acid β-oxidation is also involved in lipid metabolism, during which it produces Suc for postgermination growth (Hayashi et al., 1998). Therefore, the *ped1* mutant, which is defective in fatty acid β-oxidation, is resistant to 2,4-DB and cannot grow on medium that lacks Suc (Figure 9H). Like the *ped1* mutant, *apem9i* mutants exhibited 2,4-DB resistance (Figure 9H, top panel) and were unable to grow without exogenous Suc (Figure 9H, bottom

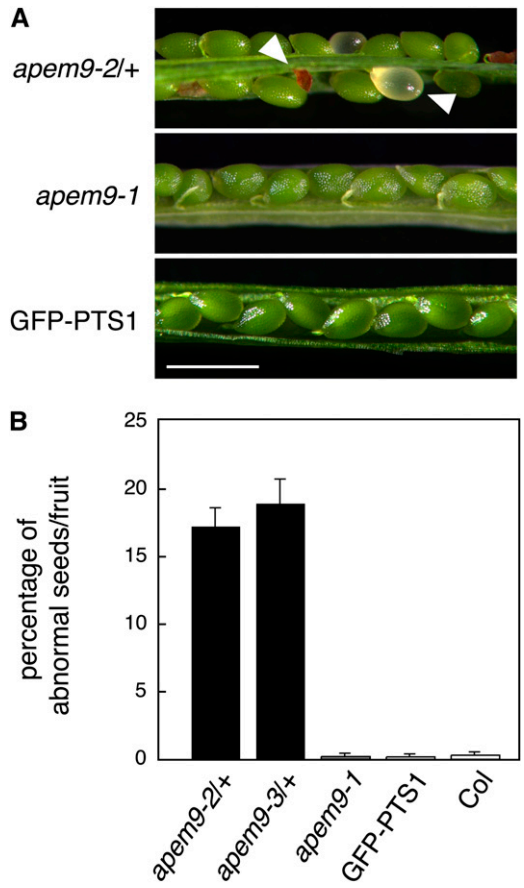

Figure 8. Seed Establishment in the T-DNA Insertion Lines.

(A) Abnormal seeds in the fruit of the T-DNA insertion line. Images show the seed set in self-fertilized fruits from *apem9-2*/+ (heterozygote), *apem9-1*, and GFP-PTS1 parental plants. White arrowheads indicate abnormal seeds. Bar = 1 mm.

(B) Proportions of abnormal seeds produced by *apem9-2*/+, *apem9-3*/+, *apem9-1*, GFP-PTS1, and wild-type (Col) plants. Data represent means ± SD (n = 10).

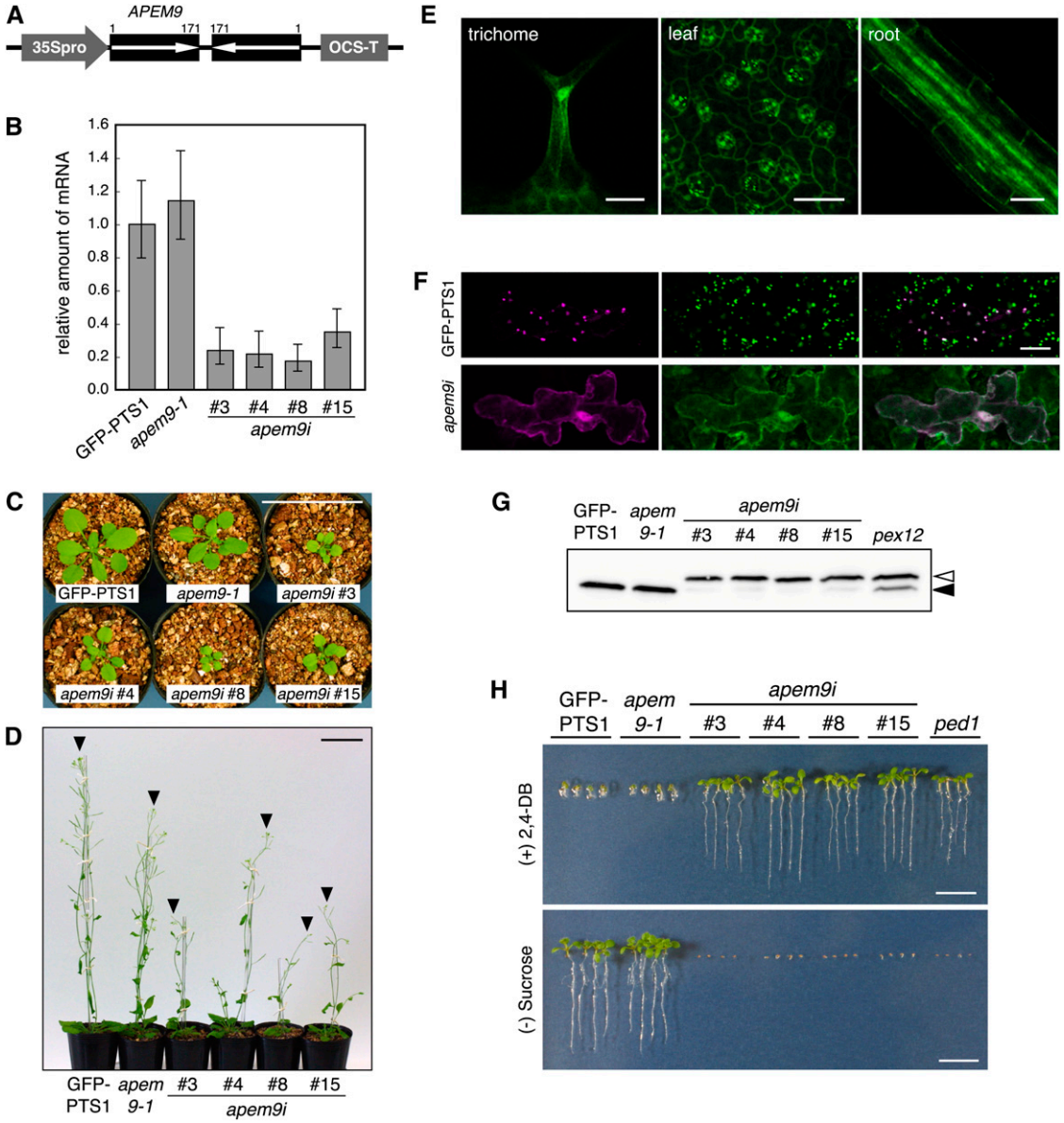

Figure 9. Analysis of the *apem9i* Knockdown Mutant.

(A) Construct for generating *apem9i* mutants. A partial cDNA fragment (1 to 171 bp) was derived from *APEM9*. 35Spro and OCS-T represent the CaMV 35S promoter and octopin synthase terminator, respectively.

(B) The amount of *APEM9* mRNA in the GFP-PTS1 plants, *apem9-1* mutants, and four independent *apem9i* mutants was estimated by quantitative RT-PCR with the TaqMan Gene Expression assay. The data were normalized with respect to *Actin 8*, and the amount of mRNA in the GFP-PTS1 plant was normalized to 1.0. Data are represented as means ± SE of three independent experiments.

(C) and **(D)** Growth phenotypes of GFP-PST1, *apem9-1* mutants, and four independent *apem9i* mutants (*apem9i* #3, #4, #8, and #15) at 3 **(C)** and 6 **(D)** weeks of age. Each arrowhead in **(D)** indicates the top of the plant. Bars = 5.0 cm.

(E) GFP fluorescence pattern of *apem9i* #3 in trichome, leaf, and root cells. Bars = 50 μm.

(F) and **(G)** Defect in PTS2-dependent transport.

(F) *PTS2-fusion mRFP1* was transiently expressed in epidermal cells of the GFP-PTS1 plants using particle bombardment. Magenta represents PTS2-mRFP1 signals. Bar = 20 μm.

(G) The polypeptides of 3-ketoacyl-CoA thiolase were immunodetected in extracts from GFP-PTS1 plants and from *apem9-1*, *apem9i*, and *pex12*/*apm4* mutants, which were grown in continuous darkness for 3 d. Arrowheads represent the positions of the precursor (open arrowhead) and mature proteins (closed arrowhead).

(H) Effects of 2,4-DB and Suc on postgermination growth. Seedlings were grown for 7 d under constant illumination on medium containing 0.35 μg mL^{-1} 2,4-DB or medium lacking Suc. Photographs were taken after the seedlings were removed from the medium and rearranged on agar plates. Bars = 1.0 cm.

panel), whereas GFP-PTS1 and *apem9-1* mutants were sensitive to 2,4-DB and did not require Suc. These results show that peroxisomal fatty acid β-oxidation activity is significantly reduced in *apem9i* mutants compared with *apem9-1* mutants.

DISCUSSION

Forward Genetics Approach Identified *APEM9*

Most eukaryotic cells contain a set of components, known as PEXs, which function in peroxisome biogenesis. *Arabidopsis* was recently also found to contain a set of *PEX* genes, which were identified based on sequence homologies (Mullen et al., 2001; Nito et al., 2007). Plant peroxisomes, however, have evolved to have plant-specific peroxisomal functions, such as phytohormone biosynthesis and photorespiration (Hayashi and Nishimura, 2006). Additionally, plant peroxisomes collaborate with chloroplasts and mitochondria during photosynthesis, photorespiration, and biosynthesis of phytohormones and exchange their metabolic derivatives (Hayashi and Nishimura, 2006). Therefore, the biogenesis and maintenance of plant peroxisomes are thought to require plant-specific systems of gene expression, transport, and substrate metabolism. To understand the mechanisms underlying the biogenesis and functions of plant peroxisomes, we screened ethyl methanesulfonate–treated transgenic *Arabidopsis* plants in which the peroxisomes were tagged with GFP (Mano et al., 2002) and identified *DYNAMIN-RELATED PROTEIN 3A*, *PEX12*, and *PEX13* as *APM1*, *APM4*, and *APM2*, respectively (Mano et al., 2004, 2006). Like *pex13*/*apm4* and *pex12*/*apm4*, *apem9-1* showed a decrease in the efficiency of protein transport; some GFP signal was detected in the cytosol and the remainder occurred in the peroxisomes (Figure 1A). In addition, T-DNA insertion lines of *APEM9* showed abnormal seed development in the fruits of the heterozygous plant and could not produce homozygous mutants (Figure 8), as were the cases for *PEX12* and *PEX13* (Fan et al., 2005; Boisson-Dernier et al., 2008). Defects in *PEX* genes are lethal in humans, causing peroxisome biogenesis disorders (Fujiki, 2000). Yeasts that lack *PEX* genes cannot survive on medium containing oleic acid as a sole carbon source that requires metabolism in peroxisomes, although can grow without peroxisomes on Glc medium (Erdmann et al., 1989; Birschmann et al., 2003). These findings indicate that most eukaryotic cells lacking one of the genes responsible for peroxisome biogenesis cannot survive. However, treatment with ethyl methanesulfonate typically causes nucleotide substitutions that result in mutants that have weaker defects than that of knockout mutants. Our forward genetics approach using the GFP-PTS1 plants is a powerful tool for identifying the critical, plant-specific factors involved in peroxisome biogenesis. Indeed, this study has successfully identified APEM9 as a novel peroxisome biogenesis factor in *Arabidopsis*.

APEM9 Is Localized to the Peroxisomal Membrane

The hydrophobic region in the C terminus of APEM9 is responsible for the predicted TMD (Figure 3A). Additionally, our microscopy observations revealed that the signal from GFP-labeled APEM9 forms ring-like structures that surround the peroxisomes (Figure 3C). A similar ring-like fluorescence pattern was observed in a study of *pex13*/*apm2* and *pex12*/*apm4*, in which the peroxisomal membrane proteins, PEX12 and PEX13, were labeled with fluorescence proteins (Mano et al., 2006). Similar to PTS1 or PTS2, which target peroxisomal matrix proteins, mPTS is known to target peroxisomal membrane proteins. This mPTS is generally located on one or two TMDs, which correspond to the PEX19 binding site (Halbach et al., 2006; Schueller et al., 2010). Because PEX19 is involved in peroxisomal membrane protein transport, it is considered to act as a receptor or chaperone for peroxisomal membrane proteins (Rottensteiner et al., 2004; Shibata et al., 2004; Schueller et al., 2010). Our BiFC assay showed that APEM9 interacts with PEX19 (Figure 5K). The counterparts of APEM9, human Pex26 and yeast Pex15p, are also reported to interact with PEX19, and two PEX19 binding sites have been identified in and around their TMDs of the C-terminal regions (Halbach et al., 2006). Considering the hydropathy profiles (Figure 3A; see Supplemental Figure 2A online), microscopy observation, and the interaction of APEM9 with PEX19, we propose the model that newly synthesized APEM9 is transported to the peroxisomal membranes via an interaction between the C-terminal region of APEM9 and PEX19.

To confirm that APEM9 is localized to the peroxisomal membrane, we tried to analyze localization of endogenous APEM9 by biochemical approach. We prepared antibodies against APEM9 and performed immunoblot analysis using protein samples extracted from whole *Arabidopsis* plants, various tissues of *Arabidopsis*, and fractionated peroxisomes. However, a polypeptide band around 37 kD, which was calculated molecular mass for APEM9, could not be detected by not only the serum, but also IgG or affinity-purified antibodies. This might be due to the low abundance of APEM9 below the detection limit. At present, therefore, we could not show peroxisomal localization of endogenous APEM9 and the direct evidence whether endogenous APEM9 is an integral peroxisomal membrane protein. These issues should be addressed in the future.

Subcellular localization of *At3g10572* gene product has been already reported as nucleolus by Koroleva et al. (2005) using *Agrobacterium tumefaciens*–mediated transient expression method in *Arabidopsis* suspension-cultured cells. However, we think that the fluorescence of GFP-At3g10572 (APEM9) in Figure 2Sb in their article is located in the aggregates, but not in the nucleolus (Figure 2Sb in Koroleva et al., 2005). We used the particle bombardment method so that we think the difference from our data is due to the difference of experimental approaches.

APEM9 Tethers the AAA-ATPase Complex to Peroxisomal Membranes

PEX1 and PEX6 are AAA-ATPase proteins that are involved in peroxisome biogenesis. An absence of PEX1 or PEX6 causes accumulation of PEX5 (the PTS1 receptor) in the peroxisomal membranes in yeast cells (Kiel et al., 2005), indicating that these AAA-ATPases export PEX5 back to the cytosol after its cargo is released into the peroxisomal matrix. In yeast and mammalian cells, these AAA-ATPases are known to be essential for peroxisomal functions (Platta et al., 2005; Tamura et al., 2006). In plants,

the homologs of both PEX1 and PEX6 have been identified, and knockdown mutants, *pex1i* and *pex6i*, were shown to exhibit defects in peroxisomal protein transport (Zolman and Bartel, 2004; Nito et al., 2007). In this study, we report that PEX1 and PEX6 interact in plant cells, as they do in yeast and mammalian cells, and that this complex is recruited to peroxisomal membranes via the interaction with APEM9 (Figure 5). These results, together with those described above, suggest that plants have recycling systems to export PEX5 back to the cytosol like mammals and yeasts and that APEM9 has a pivotal role in peroxisomal protein transport and functions as a PEX. The model shown in Figure 10 is based on our results and those of previous reports (Collins et al., 2000; Platta et al., 2007; Brown and Baker, 2008). Briefly, PEX1 forms a complex with PEX6, and APEM9 acts to tether this PEX1-PEX6 complex to the peroxisomal membrane by binding to PEX6 at a late step during protein transport. This system turned out to be required for PEX5 receptor recycling (Collins et al., 2000; Miyata and Fujiki, 2005; Platta et al., 2007). Although it has not been reported that the recycling system is present in plant cells, our data concerning APEM9 suggest the existence the similar system in plants as mammals and yeasts. Since both PTS1- and PTS2-dependent protein transport depend on PEX5 in plants (Nito et al., 2002), these efficiencies are decreased in *apem9* mutants as shown in Figures 1B, 9F, and 9G. The sequence of transport events is required for peroxisomal function; therefore, APEM9 has a crucial role in the life cycle of the plant.

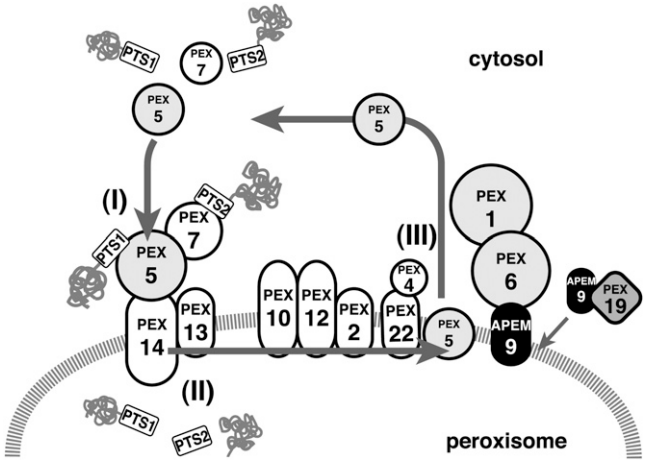

Figure 10. Working Model of Peroxisomal Protein Transport in Plants.

PTS1- or PTS2-containing proteins are directed by the PEX5-PEX7 complex from the cytosol to protein import machinery on the peroxisomal membrane, which consists of PEX14 and PEX13 (I). After protein cargoes are released inside peroxisomes (II), PEX5 is thought to be recycled to the cytosol by export machinery (III). This export machinery consists of the RING finger proteins, PEX2, PEX10, and PEX12; the E2 ubiquitin-conjugating enzyme, PEX4; PEX22; and the AAA-ATPase PEX1-PEX6 complex, which is tethered to the peroxisomal membrane by APEM9. APEM9 interacts with PEX19, which is involved in peroxisomal membrane protein transport, such that newly synthesized APEM9 is transported to the peroxisomal membrane by PEX19.

APEM9 Is a Functional Homolog of Mammal Pex26

To date, 15 PEX proteins (PEX1, 2, 3, 4, 5, 6, 7, 10, 11, 12, 13, 14, 16, 19, and 22) have been identified in plants. Because these PEXs, except for PEX22, share amino acid sequence similarities with homologs in different organisms, they could be identified by BLAST searches (Mullen et al., 2001; Nito et al., 2007). As stated above, we identified APEM9 in a mutant screening and established that it anchors PEX6 to the peroxisomal membrane. APEM9 was not previously identified by sequence comparisons; indeed, it displays limited similarity to its mammalian and yeast counterparts (identities are <20%), although there are several highly similar proteins in other plant species (see Supplemental Table 1 online). However, we found that *Arabidopsis* APEM9 is structurally similar to yeast Pex15p and mammalian Pex26, with a single predicted TMD at the C terminus and a hydrophilic region, consisting of 35 to 60 residues, just before the TMD (see Supplemental Figure 2A online).

There is a large family of Pex26 homologs in vertebrates. It is reported that Pex26 is a peroxisomal membrane protein, which anchors Pex1-Pex6 complex to peroxisomal membrane, and that its defects cause mortal effects known as peroxisome biogenesis disorders (Matsumoto et al., 2003). Pex26-dependent peroxisomal localization of Pex6 has been demonstrated using Chinese hamster ovary (CHO) cells (Matsumoto et al., 2003). In the mutant *pex26* CHO cells, Pex6 was located in the cytosol, whereas Pex6 was detected on peroxisomes when Pex26 was coexpressed. Similarly, Pex1 was barely detectable in the *pex26* CHO cells, whereas Pex1 was detected on peroxisomes in the *pex26* CHO cells expressing Pex26 and Pex6. In addition, studies in yeast cells with immunoelectron micrograph showed that exogenous Pex6p (GFP-Pex6) localization was detected on the peroxisomal membranes dependent on the amount of Pex15p, which is a counterpart of Pex26 (Birschmann et al., 2003). Considering our results together with these reports, we concluded that plants have a mechanism similar to that in mammals and yeasts.

Three iterated PSI-BLAST using *Arabidopsis* APEM9 detected mammalian Pex26 homologs, although Pex26 could not detect APEM9 in the same search. In this study, we demonstrated that the fusion protein of APEM9 with fluorescent protein (FP) showed similar behavior to Pex26 in mammalian cells; the fusion protein of APEM9 with FP can interact with PEX6 and recruit PEX6 to peroxisomal membrane (Figures 4 to 6). Additionally, subcellular localization of the fusion protein of APEM9 with FP was altered by the *apem9-1* mutation in TMD (Figure 3), which is consistent with the report that TMD of Pex26 has the information for peroxisomal localization. These results support that *Arabidopsis* APEM9 is functionally homologous to Pex26 in mammals. PEX22, identified as a PEX4 anchoring protein (Collins et al., 2000), provides another example of a conserved structure despite low sequence conservation and thereby emphasizes that plant, yeast, and mammalian proteins that perform the same functions often have structural similarities (Zolman et al., 2005).

Regarding the relationship between PEX6-APEM9 and PEX4-PEX22, we propose the following hypothesis. PEX6 and PEX4 contain a catalytic domain for AAA-ATPase and ubiquitin-conjugating activity, respectively. These activities and the

structural affinity for their substrates are indispensable for their functioning, so their amino acid sequences are relatively conserved during evolution. On the other hand, anchoring proteins, such as APEM9 and PEX22, do not require strict sequence conservation, although their transmembrane regions, which consist of hydrophobic residues, and the sites that interact with their partners should be conserved. APEM9 could not rescue the *pex15* mutant phenotype on plates containing oleate as a sole carbon source (see Supplemental Figure 2B online; Birschmann et al., 2003). Transient expression of the *GFP-Pex15p* (yeast) fusion gene in onion cells resulted in the mislocalization of Pex15p in the cytosol. This failure of yeast Pex15p to localize to peroxisomes in plant cells (see Supplemental Figure 2C online) suggests that the machinery of membrane protein targeting in plants may be different from that in yeasts.

In conclusion, we discovered that an anchoring protein for the PEX1-PEX6 complex evolved as APEM9 in plants, which is a functional homolog of mammal Pex26. APEM9 is required for the functioning of the peroxisome throughout the plant life cycle. Future work that examines the peroxisome biogenesis factors in various species will help us better understand the origin and process of the species-specific evolution of peroxisomes.

METHODS

Plant Materials and Growth Conditions

GFP-PTS1 transgenic plants and *apem* mutants were derived from the Columbia background (Mano et al., 2002, 2004). Two lines with a T-DNA insertion in the *At3g10572* locus, SALK_132193 and SALK_022380, were identified using the SIGnAL T-DNA Express: Arabidopsis Gene Mapping Tool (http://signal.salk.edu/cgi-bin/tdnaexpress; Alonso et al., 2003). Seeds of these two lines were obtained from the ABRC (http://abrc.osu.edu/), and the position of each T-DNA insertion was confirmed. These two lines were backcrossed three times with Columbia. SALK_132193 and SALK_022380 were designated *apem9-2* and *apem9-3*, respectively. To examine the relationship of the phenotype with genotype, the presence of T-DNA insertions was checked by PCR using gene-specific primers with T-DNA specific LB-1 primer (see Supplemental Table 2 online). Germination was induced by incubating the seeds for 48 h at 4°C and then transferring them to 22°C under continuous light. Seedlings were grown at 22°C on solid medium containing 2.3 mg mL^{-1} Murashige and Skoog salts (Wako), 1% Suc, 100 μg mL^{-1} myo-inositol, 1 μg mL^{-1} thiamine-HCl, 0.5 μg mL^{-1} pyridoxine-HCl, 0.5 μg mL^{-1} nicotinic acid, 0.5 μg mL^{-1} MES-KOH, pH 5.7, and 0.8% agar (INA). Two-week-old plants were transferred to soil under long-day conditions (16 h light/8 h dark) at 22°C. Most *apem9i* mutants showed severe germination defects. Therefore, all seed coats were nicked to accelerate seed coat rupturing (Footitt et al., 2006; Kanai et al., 2010).

Confocal Microscopy

Tissues from plants were examined using an LSM510META confocal laser scanning microscope (Carl Zeiss), as previously described (Mano et al., 2002). YFP fluorescence was detected using the META system (Carl Zeiss).

Map-Based Cloning and Identification of *APEM9*

apem9-1, which was backcrossed three times with the parental plant, GFP-PTS1, was crossed with another accession, Landsberg *erecta* to produce F1 and subsequently F2 progenies. A total of 296 F2 progeny expressing the *apem9-1* phenotype were scored according to their genetic background, as determined by a series of cleaved amplified polymorphic sequence and simple sequence length polymorphism markers (Konieczny and Ausubel, 1993; Bell and Ecker, 1994). Rough mapping located the *APEM9* locus between the CA1 and nga162 markers on chromosome 3. Several sets of cleaved amplified polymorphic sequence and simple sequence length polymorphism markers were made for fine mapping, according to sequences available in the Monsanto Arabidopsis Polymorphism Collection (http://www.Arabidopsis.org/browse/Cereon/). Fine mapping located the *APEM9* locus between the F13M14 and T7M13 BAC clones, which contains 33 predicted genes. The nucleotide substitution in *At3g10572* was determined as a possible candidate for the *APEM9* gene.

To confirm that the correct gene was identified, the *APEM9* genomic fragment, which includes a 1.8-kb upstream region and a 0.5-kb downstream region, was cloned into pCR8/GW/TOPO (Invitrogen), and the insert was transferred into the binary vector, pGWB1 (Nakagawa et al., 2007), using the Gateway LR recombination method (Invitrogen). The construct was transformed into *Agrobacterium tumefaciens* strain C58C1Rif^{R} and then introduced into *apem9-1* plants using the floral dip method (Clough and Bent, 1998).

Plasmid Construction

The *APEM9*, *PEX6*, and *PEX19-1* cDNA fragments, which were produced with *att*B1 and *att*B2 sequences at their 5′ and 3′ ends, respectively, were amplified by PCR with gene-specific primer sets (see Supplemental Table 2 online) and cloned into the entry vector, pDONR221 (Invitrogen), using the Gateway BP recombination method (Invitrogen). An *APEM9* cDNA clone containing the *apem9-1* point mutation (APEM9$^{[G278E]}$) was prepared by PCR-based site-directed mutagenesis with *Pfu Turbo* DNA polymerase (Stratagene) and the specific primer set (see Supplemental Table 2 online). *PEX1* cDNA was amplified using first-strand cDNA as a template and cloned into pCR8/GW/TOPO (Invitrogen) according to the manufacturer's instructions. To construct *GFP* and *TagRFP* fusion genes (Evrogen; Merzlyak et al., 2007), the cDNAs that were cloned into pDONR221 or pCR8/GW/TOPO were transferred into the destination vector pUGW6 (Nakagawa et al., 2007) to generate the GFP-fusion or into pUGW61 (kindly provided by T. Nakagawa, Shimane University) to generate the TagRFP-fusion using the Gateway LR recombination reaction. For BiFC experiments, cDNAs cloned in pDONR221 or pCR8/GW/TOPO were transferred into the destination vector nYFP/pUGW0 or cYFP/pUGW0 (kindly provided by T. Nakagawa) (Singh et al., 2009).

Generation of the *apem9i* Mutants

A construct containing a cDNA fragment in a pHELLSGATE vector (Wesley et al., 2001; Nito et al., 2007), which generates double-stranded RNA, was made using a 171-bp sequence derived from *APEM9* cDNA, which showed no significant similarity to any other *Arabidopsis thaliana* open reading frames. The 171-bp fragment of *APEM9* cDNA was amplified by PCR using a gene-specific primer set (see Supplemental Table 2 online). This RNAi construct was introduced into GFP-PTS1 plants. Transformants were selected on medium containing 10 μg mL^{-1} glufosinate-ammonium (Sigma-Aldrich). The suppression of *APEM9* mRNA accumulation was evaluated in 20 independent T3 progeny by quantitative RT-PCR. Experiments were performed using T3 progeny.

Particle Bombardment

Gold particles (1.0 μm) coated with plasmid were introduced into onion or *Arabidopsis* epidermal cells using a Helios Gene Gun (Bio-Rad) according to the manufacturer's instructions. Onion (*Allium cepa*) epidermal peels or

Arabidopsis leaves were placed on wet filter paper and used for bombardment. Bombardment was at a helium pressure of 200 p.s.i. The bombarded samples were incubated for 16 h at 22°C and were observed by LSM510 microscopy (Carl Zeiss).

mbSUS

The interaction assay using mbSUS was performed according to Grefen et al. (2007). The full-length cDNA of *PEX6*, which was cloned in pCR8/GW/TOPO (Invitrogen), was transferred into pMetYC-DEST (Grefen et al., 2007) and introduced into the haploid strain, THY.AP4. The full-length cDNAs of *APEM9*, *APEM9*$^{[G278E]}$ and *PMP38* in pDONR221 (Invitrogen), were transferred into pNX32-DEST (Grefen et al., 2007) by the Gateway LR recombination reaction (Invitrogen) and introduced into the haploid yeast strain, THY.AP5. The introduction of plasmids into yeast was confirmed by selection on plasmid-selective media and colony-direct PCR. After the transformed THY.AP4 cells were mated with the transformed THY.AP5 cells, the presence of the plasmids and the interaction between PEX6 and APEM9, APEM9$^{[G278E]}$, or PMP38 was assayed by growth on the appropriate media.

Immunoblot Analysis

For extraction of total proteins, *Arabidopsis* seedlings were homogenized with extraction buffer containing 20 mM Tris-HCl, pH 6.8, 10% β-mercaptoethanol, 2% SDS, and 24% glycerol. Homogenates were centrifuged at 20,000*g* for 10 min at 4°C, and supernatants were collected. The concentration of extracted proteins was estimated using a protein assay kit (Bio-Rad) with bovine γ-albumin as a standard. Proteins were separated by SDS-PAGE and transferred to a polyvinylidene fluoride membrane (Millipore) in a semidry electroblotting system. Immunoreactive bands were detected by monitoring the activity of a horseradish peroxidase–coupled antibody against rabbit IgG (ECL system; GE Healthcare).

Quantitative RT-PCR Analysis

Total RNA was isolated from 10-d-old seedlings using the RNeasy kit (Qiagen). First-strand cDNA was synthesized from 1 μg total RNA using Ready-To-Go RT-PCR beads (GE Healthcare). The amounts of *APEM9* mRNA were evaluated using the 7500 Fast Real-Time PCR system (Applied Biosystems). According to the manufacturer's instructions, the Absolute Quantification method was used to estimate the accumulation of *APEM9* in various tissues, using specific primer sets (see Supplemental Table 2 online). For *apem9i* mutants, the Relative Quantification method was used with the TaqMan Gene Expression assay. The identifiers are At02173897_g1 for *APEM9* and At02270958_gH for *Actin8*, respectively. The relative quantity was calculated by the $2^{-\Delta\Delta Ct}$ method (Livak and Schmittgen, 2001).

Complementation Analysis in the Yeast *pex15* Mutant

For yeast mutant complementation, a full-length cDNA clone of *APEM9* (derived from *Arabidopsis*) or *Pex15p* (derived from *Saccharomyces cerevisiae*) with the *Spe*I and *Sal*I sites was amplified by PCR using gene-specific primers (see Supplemental Table 2 online). The amplified DNA fragments were subcloned into the pT7Blue T-vector (Novagen), yielding pT7/SpeI-APEM9-SalI and pT7/SpeI-Pex15p-SalI, respectively. The *APEM9* and *Pex15p* cDNAs were digested with *Spe*I and *Sal*I and transferred into the yeast transformation vector, p416-TEF (a pRS416 derivative containing the *TEF* promoter and *URA3*), to yield p416-TEF/APEM9 and p416-TEF/Pex15p, respectively. The *S. cerevisiae pex15* deletion mutant (yol044w) was transformed with p416-TEF/APEM9, p416-TEF/Pex15p, or p416-TEF (empty vector). Wild-type strain BY4741, *pex15* mutants, and the transformants were spotted onto oleic acid medium (0.7% yeast nitrogen base without amino acids, 1× amino acids as required, 0.1% oleic acid in 0.4% Tween 40, and 2% bacto agar) to examine the peroxisomal function, as described previously (Elgersma et al., 1997).

Accession Numbers

Sequence data from this article can be found in the Arabidopsis Genome Initiative or GenBank/EMBL databases under the following accession numbers: *APEM9* (At3g10572), *PEX6* (At1g03000), *PEX1* (At5g08470), *PEX12* (At3g04460), *PMP38* (At2g39970), *PEX19-1* (At3g03490), *Homo sapiens Pex26* (Q7Z412), and *S. cerevisiae Pex15p* (Q08215). Accession numbers for homologs of *APEM9* found in other plant species are listed in Supplemental Table 1 online. The GenBank accession numbers for knockout lines mentioned in this article are SALK_132193 (*apem9-2*) and SALK_022380 (*apem9-3*).

Supplemental Data

The following materials are available in the online version of this article.

Supplemental Figure 1. Subcellular Localization of APEM9 and PEX6 in *Arabidopsis* Cells and Peroxisomal Membrane Localization of APEM9-PEX6 Complex in Onion Cells.

Supplemental Figure 2. Comparison of Hydropathy Profiles between APEM9, Pex26, and Pex15p Proteins and an Analysis of Yeast Pex15p.

Supplemental Table 1. Homologs of *Arabidopsis APEM9*.

Supplemental Table 2. Nucleotide Sequences of Primers Used in This Study.

ACKNOWLEDGMENTS

We thank T. Nakagawa for providing the Gateway vectors, R.Y. Tsien for providing the mRFP1 clone, P.M. Waterhouse for providing the pHELLSGATE8 vector, M. Hasebe for valuable comments, Y. Kamada in the Division of Molecular Cell Biology for technical supports on yeast experiments, and C. Nanba for supporting the plant growth. This study was supported in part by grants from the Japanese Ministry of Education, Sports, Culture, Science, and Technology (MEXT) to M.N. and S.M.; a Grant-in-Aid for Scientific Research of Priority Areas from MEXT on 'Organelle Differentiation as the Strategy for Environmental Adaptation in Plants'; a Grant-in-Aid for Scientific Research on Innovative Areas from MEXT on 'Environmental Sensing of Plants: Signal Perception, Processing Cellular Responses'; the Center for the Promotion of Integrated Sciences of Sokendai; and the Japan Society for the Promotion of Science for a Research Fellowship for Young Scientists to S.G.

Received October 26, 2010; revised March 7, 2011; accepted March 24, 2011; published April 12, 2011.

REFERENCES

Alonso, J.M., et al. (2003). Genome-wide insertional mutagenesis of *Arabidopsis thaliana*. Science **301:** 653–657.

Arai, Y., Hayashi, M., and Nishimura, M. (2008). Proteomic identification and characterization of a novel peroxisomal adenine nucleotide transporter supplying ATP for fatty acid β-oxidation in soybean and *Arabidopsis*. Plant Cell **20:** 3227–3240.

Babujee, L., Wurtz, V., Ma, C., Lueder, F., Soni, P., van Dorsselaer, A., and Reumann, S. (2010). The proteome map of spinach leaf peroxisomes indicates partial compartmentalization of phylloquinone

(vitamin K1) biosynthesis in plant peroxisomes. J. Exp. Bot. **61:** 1441–1453.

Bell, C.J., and Ecker, J.R. (1994). Assignment of 30 microsatellite loci to the linkage map of *Arabidopsis*. Genomics **19:** 137–144.

Birschmann, I., Stroobants, A.K., van den Berg, M., Schäfer, A., Rosenkranz, K., Kunau, W.-H., and Tabak, H.F. (2003). Pex15p of *Saccharomyces cerevisiae* provides a molecular basis for recruitment of the AAA peroxin Pex6p to peroxisomal membranes. Mol. Biol. Cell **14:** 2226–2236.

Boisson-Dernier, A., Frietsch, S., Kim, T.-H., Dizon, M.B., and Schroeder, J.I. (2008). The peroxin loss-of-function mutation *abstinence by mutual consent* disrupts male-female gametophyte recognition. Curr. Biol. **18:** 63–68.

Bracha-Drori, K., Shichrur, K., Katz, A., Oliva, M., Angelovici, R., Yalovsky, S., and Ohad, N. (2004). Detection of protein-protein interactions in plants using bimolecular fluorescence complementation. Plant J. **40:** 419–427.

Brown, L.A., and Baker, A. (2008). Shuttles and cycles: Transport of proteins into the peroxisome matrix (review). Mol. Membr. Biol. **25:** 363–375.

Clough, S.J., and Bent, A.F. (1998). Floral dip: A simplified method for *Agrobacterium*-mediated transformation of *Arabidopsis thaliana*. Plant J. **16:** 735–743.

Collins, C.S., Kalish, J.E., Morrell, J.C., McCaffery, J.M., and Gould, S.J. (2000). The peroxisome biogenesis factors Pex4p, Pex22p, Pex1p, and Pex6p act in the terminal steps of peroxisomal matrix protein import. Mol. Cell. Biol. **20:** 7516–7526.

Distel, B., et al. (1996). A unified nomenclature for peroxisome biogenesis factors. J. Cell Biol. **135:** 1–3.

Elgersma, Y., Kwast, L., van den Berg, M., Snyder, W.B., Distel, B., Subramani, S., and Tabak, H.F. (1997). Overexpression of Pex15p, a phosphorylated peroxisomal integral membrane protein required for peroxisome assembly in *S. cerevisiae*, causes proliferation of the endoplasmic reticulum membrane. EMBO J. **16:** 7326–7341.

Erdmann, R., Veenhuis, M., Mertens, D., and Kunau, W.-H. (1989). Isolation of peroxisome-deficient mutants of *Saccharomyces cerevisiae*. Proc. Natl. Acad. Sci. USA **86:** 5419–5423.

Eubel, H., Meyer, E.H., Taylor, N.L., Bussell, J.D., O'Toole, N., Heazlewood, J.L., Castleden, I., Small, I.D., Smith, S.M., and Millar, A.H. (2008). Novel proteins, putative membrane transporters, and an integrated metabolic network are revealed by quantitative proteomic analysis of Arabidopsis cell culture peroxisomes. Plant Physiol. **148:** 1809–1829.

Faber, K.N., Heyman, J.A., and Subramani, S. (1998). Two AAA family peroxins, PpPex1p and PpPex6p, interact with each other in an ATP-dependent manner and are associated with different subcellular membranous structures distinct from peroxisomes. Mol. Cell. Biol. **18:** 936–943.

Fan, J., Quan, S., Orth, T., Awai, C., Chory, J., and Hu, J. (2005). The Arabidopsis *PEX12* gene is required for peroxisome biogenesis and is essential for development. Plant Physiol. **139:** 231–239.

Footitt, S., Marquez, J., Schmuths, H., Baker, A., Theodoulou, F.L., and Holdsworth, M. (2006). Analysis of the role of COMATOSE and peroxisomal β-oxidation in the determination of germination potential in Arabidopsis. J. Exp. Bot. **57:** 2805–2814.

Fujiki, Y. (2000). Peroxisome biogenesis and peroxisome biogenesis disorders. FEBS Lett. **476:** 42–46.

Fukao, Y., Hayashi, Y., Mano, S., Hayashi, M., and Nishimura, M. (2001). Developmental analysis of a putative ATP/ADP carrier protein localized on glyoxysomal membranes during the peroxisome transition in pumpkin cotyledons. Plant Cell Physiol. **42:** 835–841.

Geisbrecht, B.V., Collins, C.S., Reuber, B.E., and Gould, S.J. (1998). Disruption of a PEX1-PEX6 interaction is the most common cause of the neurologic disorders Zellweger syndrome, neonatal adrenoleukodystrophy, and infantile Refsum disease. Proc. Natl. Acad. Sci. USA **95:** 8630–8635.

Grefen, C., Lalonde, S., and Obrdlik, P. (2007). Split-ubiquitin system for identifying protein-protein interactions in membrane and full-length proteins. Curr. Protoc. Neurosci. **41:** 5.27.1–5.27.41.

Halbach, A., Landgraf, C., Lorenzen, S., Rosenkranz, K., Volkmer-Engert, R., Erdmann, R., and Rottensteiner, H. (2006). Targeting of the tail-anchored peroxisomal membrane proteins PEX26 and PEX15 occurs through C-terminal PEX19-binding sites. J. Cell Sci. **119:** 2508–2517.

Hayashi, M., and Nishimura, M. (2006). *Arabidopsis thaliana*—A model organism to study plant peroxisomes. Biochim. Biophys. Acta **1763:** 1382–1391.

Hayashi, M., Nito, K., Takei-Hoshi, R., Yagi, M., Kondo, M., Suenaga, A., Yamaya, T., and Nishimura, M. (2002). Ped3p is a peroxisomal ATP-binding cassette transporter that might supply substrates for fatty acid β-oxidation. Plant Cell Physiol. **43:** 1–11.

Hayashi, M., Toriyama, K., Kondo, M., and Nishimura, M. (1998). 2,4-Dichlorophenoxybutyric acid-resistant mutants of *Arabidopsis* have defects in glyoxysomal fatty acid β-oxidation. Plant Cell **10:** 183–195.

Hu, J.P., Aguirre, M., Peto, C., Alonso, J., Ecker, J., and Chory, J. (2002). A role for peroxisomes in photomorphogenesis and development of *Arabidopsis*. Science **297:** 405–409.

Huhse, B., Rehling, P., Albertini, M., Blank, L., Meller, K., and Kunau, W.H. (1998). Pex17p of *Saccharomyces cerevisiae* is a novel peroxin and component of the peroxisomal protein translocation machinery. J. Cell Biol. **140:** 49–60.

Kamada, T., Nito, K., Hayashi, H., Mano, S., Hayashi, M., and Nishimura, M. (2003). Functional differentiation of peroxisomes revealed by expression profiles of peroxisomal genes in *Arabidopsis thaliana*. Plant Cell Physiol. **44:** 1275–1289.

Kamada-Nobusada, T., Hayashi, M., Fukazawa, M., Sakakibara, H., and Nishimura, M. (2008). A putative peroxisomal polyamine oxidase, AtPAO4, is involved in polyamine catabolism in *Arabidopsis thaliana*. Plant Cell Physiol. **49:** 1272–1282.

Kamigaki, A., Kondo, M., Mano, S., Hayashi, M., and Nishimura, M. (2009). Suppression of peroxisome biogenesis factor 10 reduces cuticular wax accumulation by disrupting the ER network in *Arabidopsis thaliana*. Plant Cell Physiol. **50:** 2034–2046.

Kanai, M., Nishimura, M., and Hayashi, M. (2010). A peroxisomal ABC transporter promotes seed germination by inducing pectin degradation under the control of *ABI5*. Plant J. **62:** 936–947.

Kato, A., Hayashi, M., Takeuchi, Y., and Nishimura, M. (1996). cDNA cloning and expression of a gene for 3-ketoacyl-CoA thiolase in pumpkin cotyledons. Plant Mol. Biol. **31:** 843–852.

Khan, B.R., and Zolman, B.K. (2010). *pex5* Mutants that differentially disrupt PTS1 and PTS2 peroxisomal matrix protein import in Arabidopsis. Plant Physiol. **154:** 1602–1615.

Kiel, J.A.K.W., Emmrich, K., Meyer, H.E., and Kunau, W.-H. (2005). Ubiquitination of the peroxisomal targeting signal type 1 receptor, Pex5p, suggests the presence of a quality control mechanism during peroxisomal matrix protein import. J. Biol. Chem. **280:** 1921–1930.

Konieczny, A., and Ausubel, F.M. (1993). A procedure for mapping *Arabidopsis* mutations using co-dominant ecotype-specific PCR-based markers. Plant J. **4:** 403–410.

Koroleva, O.A., Tomlinson, M.L., Leader, D., Shaw, P., and Doonan, J.H. (2005). High-throughput protein localization in Arabidopsis using *Agrobacterium*-mediated transient expression of GFP-ORF fusions. Plant J. **41:** 162–174.

Kragler, F., Lametschwandtner, G., Christmann, J., Hartig, A., and Harada, J.J. (1998). Identification and analysis of the plant

peroxisomal targeting signal 1 receptor NtPEX5. Proc. Natl. Acad. Sci. USA **95:** 13336–13341.

Lin, Y., Sun, L., Nguyen, L.V., Rachubinski, R.A., and Goodman, H.M. (1999). The Pex16p homolog SSE1 and storage organelle formation in *Arabidopsis* seeds. Science **284:** 328–330.

Livak, K.J., and Schmittgen, T.D. (2001). Analysis of relative gene expression data using real-time quantitative PCR and the $2^{-\Delta\Delta Ct}$ method. Methods **25:** 402–408.

Ludewig, U., Wilken, S., Wu, B., Jost, W., Obrdlik, P., El Bakkoury, M., Marini, A.M., André, B., Hamacher, T., Boles, E., von Wirén, N., and Frommer, W.B. (2003). Homo- and hetero-oligomerization of ammonium transporter-1 $NH4^+$ uniporters. J. Biol. Chem. **278:** 45603–45610.

Mano, S., Nakamori, C., Hayashi, M., Kato, A., Kondo, M., and Nishimura, M. (2002). Distribution and characterization of peroxisomes in Arabidopsis by visualization with GFP: Dynamic morphology and actin-dependent movement. Plant Cell Physiol. **43:** 331–341.

Mano, S., Nakamori, C., Kondo, M., Hayashi, M., and Nishimura, M. (2004). An *Arabidopsis* dynamin-related protein, DRP3A, controls both peroxisomal and mitochondrial division. Plant J. **38:** 487–498.

Mano, S., Nakamori, C., Nito, K., Kondo, M., and Nishimura, M. (2006). The Arabidopsis *pex12* and *pex13* mutants are defective in both PTS1- and PTS2-dependent protein transport to peroxisomes. Plant J. **47:** 604–618.

Matsumoto, N., Tamura, S., and Fujiki, Y. (2003). The pathogenic peroxin Pex26p recruits the Pex1p-Pex6p AAA ATPase complexes to peroxisomes. Nat. Cell Biol. **5:** 454–460.

Meinecke, M., Cizmowski, C., Schliebs, W., Krüger, V., Beck, S., Wagner, R., and Erdmann, R. (2010). The peroxisomal importomer constitutes a large and highly dynamic pore. Nat. Cell Biol. **12:** 273–277.

Merzlyak, E.M., Goedhart, J., Shcherbo, D., Bulina, M.E., Shcheglov, A.S., Fradkov, A.F., Gaintzeva, A., Lukyanov, K.A., Lukyanov, S., Gadella, T.W., and Chudakov, D.M. (2007). Bright monomeric red fluorescent protein with an extended fluorescence lifetime. Nat. Methods **4:** 555–557.

Miyata, N., and Fujiki, Y. (2005). Shuttling mechanism of peroxisome targeting signal type 1 receptor Pex5: ATP-independent import and ATP-dependent export. Mol. Cell. Biol. **25:** 10822–10832.

Mullen, R.T., Flynn, C.R., and Trelease, R.N. (2001). How are peroxisomes formed? The role of the endoplasmic reticulum and peroxins. Trends Plant Sci. **6:** 256–261.

Nair, D.M., Purdue, P.E., and Lazarow, P.B. (2004). Pex7p translocates in and out of peroxisomes in *Saccharomyces cerevisiae*. J. Cell Biol. **167:** 599–604.

Nakagawa, T., Kurose, T., Hino, T., Tanaka, K., Kawamukai, M., Niwa, Y., Toyooka, K., Matsuoka, K., Jinbo, T., and Kimura, T. (2007). Development of series of gateway binary vectors, pGWBs, for realizing efficient construction of fusion genes for plant transformation. J. Biosci. Bioeng. **104:** 34–41.

Nishimura, M., Takeuchi, Y., De Bellis, L., and Hara-Nishimura, I. (1993). Leaf peroxisomes are directly transformed to glyoxysomes during senescence of pumpkin cotyledons. Protoplasma **175:** 131–137.

Nito, K., Hayashi, M., and Nishimura, M. (2002). Direct interaction and determination of binding domains among peroxisomal import factors in *Arabidopsis thaliana*. Plant Cell Physiol. **43:** 355–366.

Nito, K., Kamigaki, A., Kondo, M., Hayashi, M., and Nishimura, M. (2007). Functional classification of *Arabidopsis* peroxisome biogenesis factors proposed from analyses of knockdown mutants. Plant Cell Physiol. **48:** 763–774.

Obrdlik, P., et al. (2004). K^+ channel interactions detected by a genetic system optimized for systematic studies of membrane protein interactions. Proc. Natl. Acad. Sci. USA **101:** 12242–12247.

Platta, H.W., El Magraoui, F., Schlee, D., Grunau, S., Girzalsky, W., and Erdmann, R. (2007). Ubiquitination of the peroxisomal import receptor Pex5p is required for its recycling. J. Cell Biol. **177:** 197–204.

Platta, H.W., and Erdmann, R. (2007). The peroxisomal protein import machinery. FEBS Lett. **581:** 2811–2819.

Platta, H.W., Grunau, S., Rosenkranz, K., Girzalsky, W., and Erdmann, R. (2005). Functional role of the AAA peroxins in dislocation of the cycling PTS1 receptor back to the cytosol. Nat. Cell Biol. **7:** 817–822.

Preisig-Müller, R., and Kindl, H. (1993). Thiolase mRNA translated *in vitro* yields a peptide with a putative N-terminal presequence. Plant Mol. Biol. **22:** 59–66.

Rehling, P., Skaletz-Rorowski, A., Girzalsky, W., Voorn-Brouwer, T., Franse, M.M., Distel, B., Veenhuis, M., Kunau, W.H., and Erdmann, R. (2000). Pex8p, an intraperoxisomal peroxin of *Saccharomyces cerevisiae* required for protein transport into peroxisomes binds the PTS1 receptor pex5p. J. Biol. Chem. **275:** 3593–3602.

Reumann, S., Babujee, L., Ma, C., Wienkoop, S., Siemsen, T., Antonicelli, G.E., Rasche, N., Lüder, F., Weckwerth, W., and Jahn, O. (2007). Proteome analysis of *Arabidopsis* leaf peroxisomes reveals novel targeting peptides, metabolic pathways, and defense mechanisms. Plant Cell **19:** 3170–3193.

Reumann, S., Ma, C.L., Lemke, S., and Babujee, L. (2004). AraPerox. A database of putative Arabidopsis proteins from plant peroxisomes. Plant Physiol. **136:** 2587–2608.

Rottensteiner, H., Kramer, A., Lorenzen, S., Stein, K., Landgraf, C., Volkmer-Engert, R., and Erdmann, R. (2004). Peroxisomal membrane proteins contain common Pex19p-binding sites that are an integral part of their targeting signals. Mol. Biol. Cell **15:** 3406–3417.

Schueller, N., Holton, S.J., Fodor, K., Milewski, M., Konarev, P., Stanley, W.A., Wolf, J., Erdmann, R., Schliebs, W., Song, Y.H., and Wilmanns, M. (2010). The peroxisomal receptor Pex19p forms a helical mPTS recognition domain. EMBO J. **29:** 2491–2500.

Schumann, U., Wanner, G., Veenhuis, M., Schmid, M., and Gietl, C. (2003). AthPEX10, a nuclear gene essential for peroxisome and storage organelle formation during Arabidopsis embryogenesis. Proc. Natl. Acad. Sci. USA **100:** 9626–9631.

Shibata, H., Kashiwayama, Y., Imanaka, T., and Kato, H. (2004). Domain architecture and activity of human Pex19p, a chaperone-like protein for intracellular trafficking of peroxisomal membrane proteins. J. Biol. Chem. **279:** 38486–38494.

Singh, T., Hayashi, M., Mano, S., Arai, Y., Goto, S., and Nishimura, M. (2009). Molecular components required for the targeting of PEX7 to peroxisomes in *Arabidopsis thaliana*. Plant J. **60:** 488–498.

Sparkes, I.A., Brandizzi, F., Slocombe, S.P., El-Shami, M., Hawes, C., and Baker, A. (2003). An Arabidopsis *pex10* null mutant is embryo lethal, implicating peroxisomes in an essential role during plant embryogenesis. Plant Physiol. **133:** 1809–1819.

Tamura, S., Yasutake, S., Matsumoto, N., and Fujiki, Y. (2006). Dynamic and functional assembly of the AAA peroxins, Pex1p and Pex6p, and their membrane receptor Pex26p. J. Biol. Chem. **281:** 27693–27704.

Wain, R.L., and Wightman, F. (1954). The growth regulating activity of certain ω-substituted alkyl carboxylic acids in relation to their β-oxidation within the plant. Proc. R. Soc. Lond. B Biol. Sci. **142:** 525–536.

Wesley, S.V., et al. (2001). Construct design for efficient, effective and high-throughput gene silencing in plants. Plant J. **27:** 581–590.

Zolman, B.K., and Bartel, B. (2004). An Arabidopsis indole-3-butyric acid-response mutant defective in PEROXIN6, an apparent ATPase implicated in peroxisomal function. Proc. Natl. Acad. Sci. USA **101:** 1786–1791.

Zolman, B.K., Monroe-Augustus, M., Silva, I.D., and Bartel, B. (2005). Identification and functional characterization of *Arabidopsis* PEROXIN4 and the interacting protein PEROXIN22. Plant Cell **17:** 3422–3435.

Zolman, B.K., Yoder, A., and Bartel, B. (2000). Genetic analysis of indole-3-butyric acid responses in *Arabidopsis thaliana* reveals four mutant classes. Genetics **156:** 1323–1337.